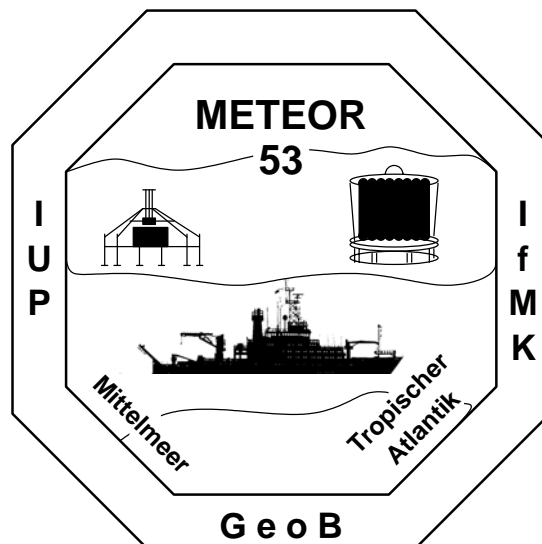


METEOR-Berichte 03-  
Circulation and Particle Fluxes  
Mediterranean – Canary – Tropical Atlantic – Caribbean  
Part 3  
Cruise No. 53, Leg 3  
7 June – 5 July 2002, Recife – Pointe a Pitre



M.Rhein, C.Mertens, R.Steinfeldt, M.Walter, G.Fraas, K. Bulsiewicz, W.T. Ochsenhirt,  
Oliver Beekmann, A.C. da Rochas, F. Geber, M. Bleischwitz, K.Kirchner, A.Moll,  
A.Schramm, T.Stadtlaender, M.Stolpmann, W.Steinbaum, F.Zeytouni, Thierry Terre

Editorial Assistance:  
Frank Schmieder  
Fachbereich Geowissenschaften, Universität Bremen

Leitstelle METEOR  
Institut für Meereskunde der Universität Hamburg

**Table of Contents (M53/3)**

3.1 Participants	3-3
3.2 Research Program	3-5
3.3 Narrative of the cruise	3-7
3.4 Preliminary Results	3-12
3.4.1 CTD-Oxygen measurements	3-12
3.4.2 CFC measurements	3-13
3.4.3 Direct Current measurements	3-13
3.4.4 The warm upper limb of the MOC	3-15
3.4.5 Contribution of southern hemispheric water	3-18
3.4.6 Velocity measurements in the Caribbean passages	3-21
3.4.7 The cold limb of the MOC	3-22
3.4.8 CFC-derived ages of NADW	3-25
3.4.9 Arrival of new LSW at 16°N	3-27
3.4.10 Mooring Activities	3-28
3.5 Weather conditions during M53/3	3-29
3.6 References	3-30
3.7 Station list and moorings M53/3	3-32

### 3.2 Participants METEOR 53-3

1.	Rhein, Monika, Prof.Dr.	chief scientist	IUP
2.	Beekmann, Oliver	oxygen analysis	IUP
3.	Bleischwitz, Marc	CFCs	IUP
4.	Bulsiewicz, Klaus	CFC analysis	IUP
5.	Fraas, Gerd	CTD/moorings	IUP
6.	Geber, Fabio	scientif.partner, Brazil	CTG/UFPP
7.	Ana Catalina da Rochas	scientif.partner, Brazil	IO/USP
8.	Kandler, Rebecca	CTD/ADCP watch	IUP
9.	Kirchner, Kerstin	CTD/ADCP watch	IUP
10.	Mertens, Christian, Dr.	data analysis, ADCPs	IUP
11.	Moll, Alexander	CFCs	IUP
12.	Ochsenhirt, Wolf-Thilo	weather technician	DWD
13.	Schramm, Angela	CTD/ADCP watch	IUP
14.	Stadtländer, Timo	mooring/CTD watch	IUP
15.	Stolpmann, Mareike	CTD/ADCP watch	IUP
16.	Steinbaum, Wibke	CTD/ADCP watch	IUP
17.	Steinfeld, Reiner, Dr.	data analysis/salinometry	IUP
18.	Zeytouni, Fereshteh	CTD/ADCP watch	IUP
19.	Terre, Thierry	Tomography moorings	IFREMER
20.	Guilherme, Angelo de Isabel	observer	Brazil

#### CTG/UFPP

Centro de Technologica e Geosciencias, Universidade Federal de Pernambuco, Recife, Brazil

#### DWD

Deutscher Wetterdienst, Geschäftsfeld Seeschifffahrt, Bernhard-Nocht-Straße 76, 20359 Hamburg, Germany

#### IFREMER

Department Geosciences Marines, IFREMER, Center de Brest, Plouzane, France

#### IO/USP

Instituto Oceanografico, Universidade de São Paulo, Praça do Oceanografico, 191, Cidade Universitaria São Paulo, CEP 05508-900, Brazil

**IUP**

Universität Bremen, Institut für Umweltphysik, Abt. Ozeanographie, Otto Hahn Allee, 28359 Bremen, Germany

### 3.2 Research Program

The thermohaline circulation (THC) and especially the meridional heat transport of the THC plays an important role for climate and climate change. In the Atlantic the THC consists of a northward transport of warm water in the upper ocean and a southward transport of cold deep water. The transports occur mainly in western boundary currents, but along the boundary currents complex recirculation cells exist with different horizontal extensions, intensities and fluctuations. These have an impact on the THC.

The cold branch of the THC transports North Atlantic Deep Water (NADW). NADW has several components with different water mass characteristics. They are formed by convection and by overflow processes and entrainment. Two of the NADW components, the water formed in the Labrador Sea and the lower deep water overflowing the Denmark Strait are marked by CFC maxima. The CFC signal is caused by the intimate contact of these water masses with the surface layer of the ocean and they might be most sensitive to climate change. Below the NADW, one finds the Antarctic Bottom Water (AABW) flowing into the North Atlantic through the Equatorial channel.

Transport estimates in the subtropical deep western boundary current showed that the transport seems to be 2-3 times higher than the assumed net transport of the THC. This led to the assumption that a deep recirculation cell exists in the the Guiana Basin. There are uncertainties about the horizontal extension, strength, and variability of this cell. Former CFC observations along 44°W could not confirm the northwestward branch along the MAR. Model calculations, however, showed that the observed tracer distributions could be simulated by an assumed recirculation in the interior of the basin. There are also indications that part of the lower NADW leaves the western basin through fracture zones of the MAR south of the Vema Fracture zone. One of the most promising passages, the 7°30'N passage, will be studied by deploying moored current meters and T-S sensors (DFG project 'West-East Passages').

The warm branch of the THC consists of warm water of South Atlantic origin. The water crosses the equator mainly in the North Brasil Undercurrent and in the South Equatorial Current. Both currents meet between 35°W and 40°W to form the northwestward flowing North Brasil Current (NBC). North of the NBC-NECC retroflexion, the northward transport occurs through eddies, and the transport are difficult to estimate.

The transport of the NBC is much higher than the net interhemispheric transport, since part of the NBC flows back into the South Atlantic with the equatorial current system. The equatorial Atlantic shows significant transport fluctuations and divergences of the wind field, so that the net exchange between the two hemisphere is difficult to estimate. Ultimately, the remaining southern Atlantic water flows into the Caribbean, and the main part of the inflow through the passages south of Gwa deloupe consists of water from southern origin. After crossing the Caribbean, the southern hemispheric water joins the Florida Current. Owing to the lack of time series, the inflow is still not known. Northern and southern water can be separated by their different T-S-O<sub>2</sub> characteristic. The planned measurements during M53/3 will give valuable information for the mooring array planned to deploy in 2003 covering the passages south of Guadeloupe.

The main objectives of M53/3 were

- estimate time scales and spreading path of recently formed deep water in the subtropical and tropical Atlantic
- estimate location and horizontal extension of the deep recirculation cell in the Guiana basin
- estimate deep water transport from the western into eastern Atlantic through the 7°30'N passages and its role for the recirculation in the Guiana basin
- determine the stratification and circulation along the MOVE array at 16°N and the water mass characteristic and the velocity field of the Caribbean inflow
- Methods used are vm-ADCP and an ADCP attached to the CTD system (IADCP). To study the stratification and the water masses, CTD, oxygen and CFC distributions will be measured. The CFC data give also information about time scales of spreading from the formation region to the subtropical/tropical Atlantic.

### 3.3 Narrative of the Cruise

In Recife, several meetings and events took place on RV Meteor between, June 3 – June 6, which were related to the ‚Jahr der Geowissenschaften‘ (Year of the Geoscience) in Germany. The Meteor left Recife on June 7, 12 UTC and headed north and then northwest to reach the southern end of the 40°W section at 2°07'S, 40°00'W. Due to favorable winds and the North Brazil Current NBC, the speed of the Meteor was about 13kn. A test station was carried out successfully on June 8.

Station work began on June 9, 13 UTC at 2°07'S, 40°00'W, water depth: 1200m. The CTD measures the vertical profile of pressure, temperature, conductivity and oxygen. Conductivity and oxygen are calibrated on board by analysing water samples taken with 21 10liter bottles. Oxygen was analysed by automatic titration and with two optical frequencies, and the salinity was determined with an Autosal. Samples taken from the water bottles were also analysed on board for the chlorofluorocarbon components CFC-11 and CFC-12 by an automatic GC-ECD system designed at the University Bremen. The CFCs are a major tool to estimate time scales of spreading of deep and intermediate water masses and to follow the spreading paths. A 150kHz narrow band IADCP is attached to the CTD-rosette system and measures the velocity profile from the surface to the bottom. The current field in the upper 1400m was continuously measured by two ADCPs: a 75 kHz and a 38 kHz ADCP Ocean Surveyor, located in the ship's hull and sea chest, respectively. The thermosalinograph records continuously the surface salinity, and was calibrated on station against the CTD values.

The distance between the CTD/IADCP stations were 5 miles at the continental slope to resolve the deep current field and increased to 25 miles north of 1°16'S, 40°N. The RV METEOR left the 200nm zone of Brazil at 0°30'N, 40°00'W on June 11, 1 UTC. At 2°30'N, 40°W, the station spacing increased to 30 miles.. At 6°N, 40°W on June 13, 17UTC the Meteor headed towards the eastern entrance of the 7°30'N fracture zone at the Midatlantic Ridge at 38°20'W. After CTD/IADCP station 22, the 4 releasers for the passage moorings were successfully tested after lowering them to 1000m depth.

In the fracture zone, CTD/IADCP work continued along 7°30'N roughly every 30 miles. On CTD/IADCP station 25, 7°26'N, 38°19.3'W, at June 14, 16 out of 21 water bottles didn't close. Despite several attempts to repair and/or to exchange part of the equipment, the malfunction could not be found. The following stations 26-29 were run without water bottles and thus without CFC samples. On CTD/IADCP station 29, June 15, 12:30UTC, no CTD data were transferred due to malfunctions of the electric cable and the SBE assembly board. After repairing both, the system was back to function normally.

On June 15, 9:30UTC the topography around the mooring location at 7°28'N, 36°52'W was surveyed with Hydrosweep. The Bremen mooring B1 was deployed at the sill in the 7°30'N passage at 7°28.40'N, 36°50.00'W, at 16:06 UTC. The mooring is equipped with pressure, temperature and conductivity sensors (MicroCats) and acoustic current meters (Aanderaa), and encompass the INADW from the bottom to about 3600m depth. The water depth at the sill turned out to be 200m deeper (4500m) than anticipated from the Sandwell-Topography (2min resolution).

On June 15, 19 UTC the ‚Meteor‘ arrived in the area, where the 2<sup>nd</sup> deployment was planned (8°00'N, 36°00'W). The topography of the area was surveyed with Hydrosweep. The deep passage (4300m depth) present in the Sandwell topography, was only 3900m deep, too shallow for a substantial INADW export. Thus we continued to follow the deep passage towards the east till 7°24.85'N, 34°19.84'W, the easternmost exit of the 7°30'N passage to

the eastern Atlantic. On June, 16, 9UTC, Hydrosweep showed, that the sill was located about 2 miles further east than found in the map and was deeper (sill depth: 4660m instead of 4200m) and the passage was wider than found in the Sandwell topography. After a CTD/IADCP station near the allocated mooring position at the sill, the Bremen mooring B2 was deployed at 7°24.70'N, 34°17.30'W at 15 UTC. At 16:30 UTC, the Bremen CFC sampler was tested for the first time by putting the device in 2000m depth for 6 hours. The moored sampler was developed in Bremen by modifying a commercially available nutrient sampler for the measurements of CFCs in deep water. The main purpose is to obtain year long time series of CFC concentrations in deep water. At 23:30, the sampler was retrieved and the METEOR headed northwestward towards the easternmost station of the 16°N section. On the way, at June, 18, 17UTC the CFC sampler was lowered to 10m depth for 90 minutes for another test. In both tests, the sampler showed no contamination affecting the analysis of CFCs.

The METEOR arrived at the eastern starting point of the 16N section (15°14'N, 51°21'W) on June 21, 2UTC. Since the IADCP can only be lowered to 5000m depth, and the bottom of the ocean is deeper than 5000m west of 52°W, two different CTD/rosette systems were used alternatively. One system (S1) with the IADCP attached was only lowered to 5000m, and on the next station, the second CTD/rosette system without IADCP (S2) was used and lowered to the bottom. The CTD station spacing is 20miles, i.e. a IADCP profile is obtained every 40 nautical miles. On CTD station 36 (15°27'N, 53°07'W, June, 22, 0UTC), the measurements were aborted in 1800m depth due to a malfunction of the conductivity sensor in S1, and the profile was repeated with S2. The conductivity sensor in S1 was replaced. On June 24, another CFC sampler test was carried out by lowering the sampler to 2500m depth for 8 hours. After recovery, the sampler was still working.

On 17 UTC, we began with the recovery of the tomography mooring m2, located at 16°02'N, 56°55'W. Both releasers responded, and were hauled on deck at 20:30 UTC. Then the RV Meteor continued CTD station work at 15°54'N, 57°00'W. The distance between the stations 54 and 56 increased to 30 miles. On June, 26, the tomography mooring m3 at 16°23'N, 60°28'W was recovered successfully. After reaching the steep continental slope off Guadeloupe, the CTD station spacing between profiles 57-63 were reduced from 15 miles to roughly 2 to 3 miles, so that the bottom depths between subsequent stations did not differ by more than 600m. The tomography mooring m5-sara at 16°22'N, 60°42'W was recovered without any problems on June 27, 18UTC.

The last task of the cruise is to measure the properties of the water masses flowing into the Caribbean Sea and to estimate their transport. The 'Meteor' headed south of Guadeloupe to the 100m isobath at 16°00.0'N, 61°34.5'W and crossed the Guadeloupe-Dominica Passage to the 100m isobath north of Dominica at 15°39'40'N, 61°26.3'W in order to measure the velocity distribution with the two vessel mounted Ocean Surveyors. It turned out that the increasing winds (Bft 8) and the waves decreased the data quality of the 38kHz system, the quality of the 75kHz ADCP mounted in the ship's hull was not affected and had good data down to 750m depth. At June, 28, on the way back to Guadeloupe, 5 CTD stations (CTD 64-68) were carried out and on the way south, the ADCPs recorded the velocity distribution in the passage for the third time. Dominica was passed leeward and the Dominica – Martinique passage was surveyed after the same fashion as the Guadeloupe-Dominica passage starting at 15°14.10'N, 61°17.70'W till 14°55.20'N, 61°08.35'W at the northern tip of Martinique (CTD stations 69-72). At the center of the passage, the water depth exceeded 2000m, and the CFC sampler was lowered for 9 hours to about 2000m to test some parameter settings. On June, 29, 16 UTC, the Meteor headed south to the Martinique – Saint Lucia passage to the northern starting location of the ADCP section at 14°22.35'N, 60°52.30'W. After finishing the ADCP section off Saint Lucia at 14°10.00'N, 60°54.30'W, 5 CTD stations (CTD stations 73-79)

were carried out along this section on the way north. After repeating the ADCP section southward, the work continued in the Saint Lucia – Saint Vincent passage with an ADCP section ( $13^{\circ}39.40'N$ ,  $60^{\circ}54.00'W$  to  $13^{\circ}21.60'N$ ,  $61^{\circ}07.00'W$ ). Since we expected the largest transport here, the ADCP section was repeated 4 times. 6 CTD stations (81-85) were carried out in the passage starting at June 30, 10 UTC. The work in the Saint Lucia - Saint Vincent passage was finished at 20 UTC. The water mass characteristic and the inflow into the Caribbean south of Saint Vincent were measured on the way from Saint Vincent to Tobago. Station spacing was 15 miles. The data quality of the 38kHz Ocean Surveyor was deteriorated severely during that section.

The stations 88 – 93 were done with the IADCP attached to the rosette. The Meteor reached the 1000m isobath off Tobago at July, 15 UTC. The stations on the way north towards Guadeloupe were about 15 miles apart. The last CTD station was done at  $16^{\circ}N$ ,  $60^{\circ}41'W$  on July, 3. The remaining time was used to repeat with ADCP measurements the  $16^{\circ}N$  boundary current section to  $59^{\circ}30'W$  in order to have another transport estimate. The research cruise M53-3 ended in Pointe a Pitre at July 4, 13 UTC. On July 5, a reception on RV Meteor was given to present the research vessel and the science to the public.

**Figure 3-1 a)** Overview cruise track of research cruise M53-3. The moorings B1 and B2 located in the  $7^{\circ}30'N$  passage are shown with red marks. **b)** Cruise track, Caribbean passages and the regions east.

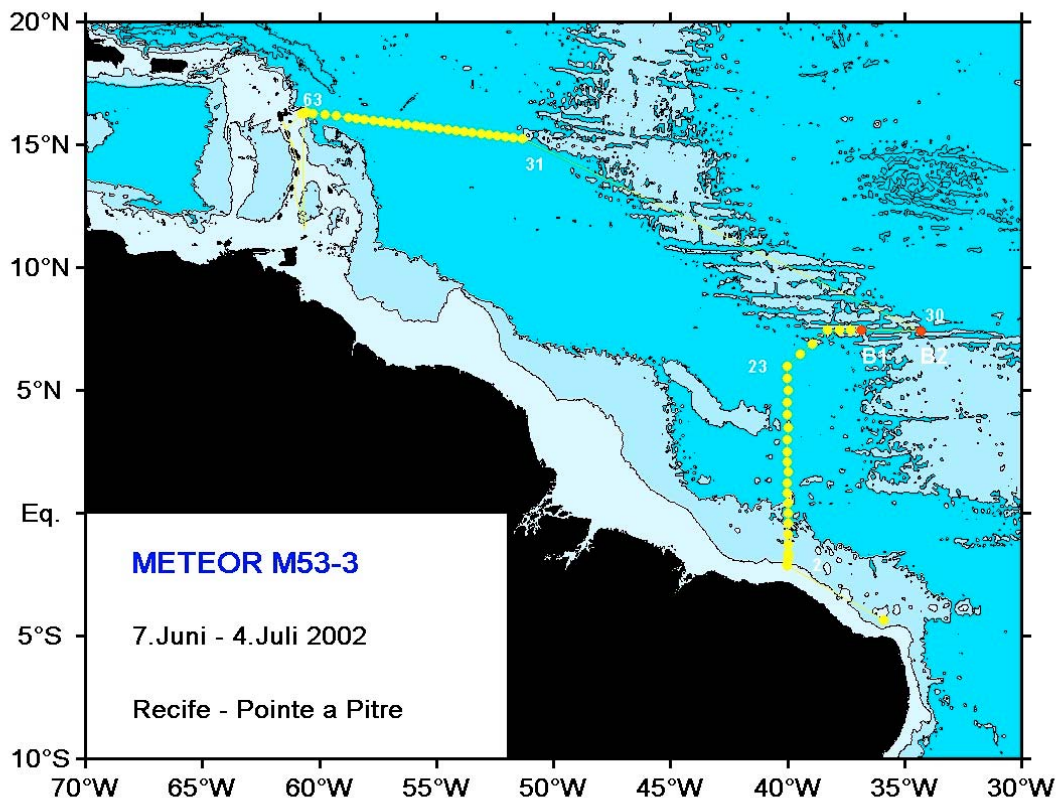


Figure 1a

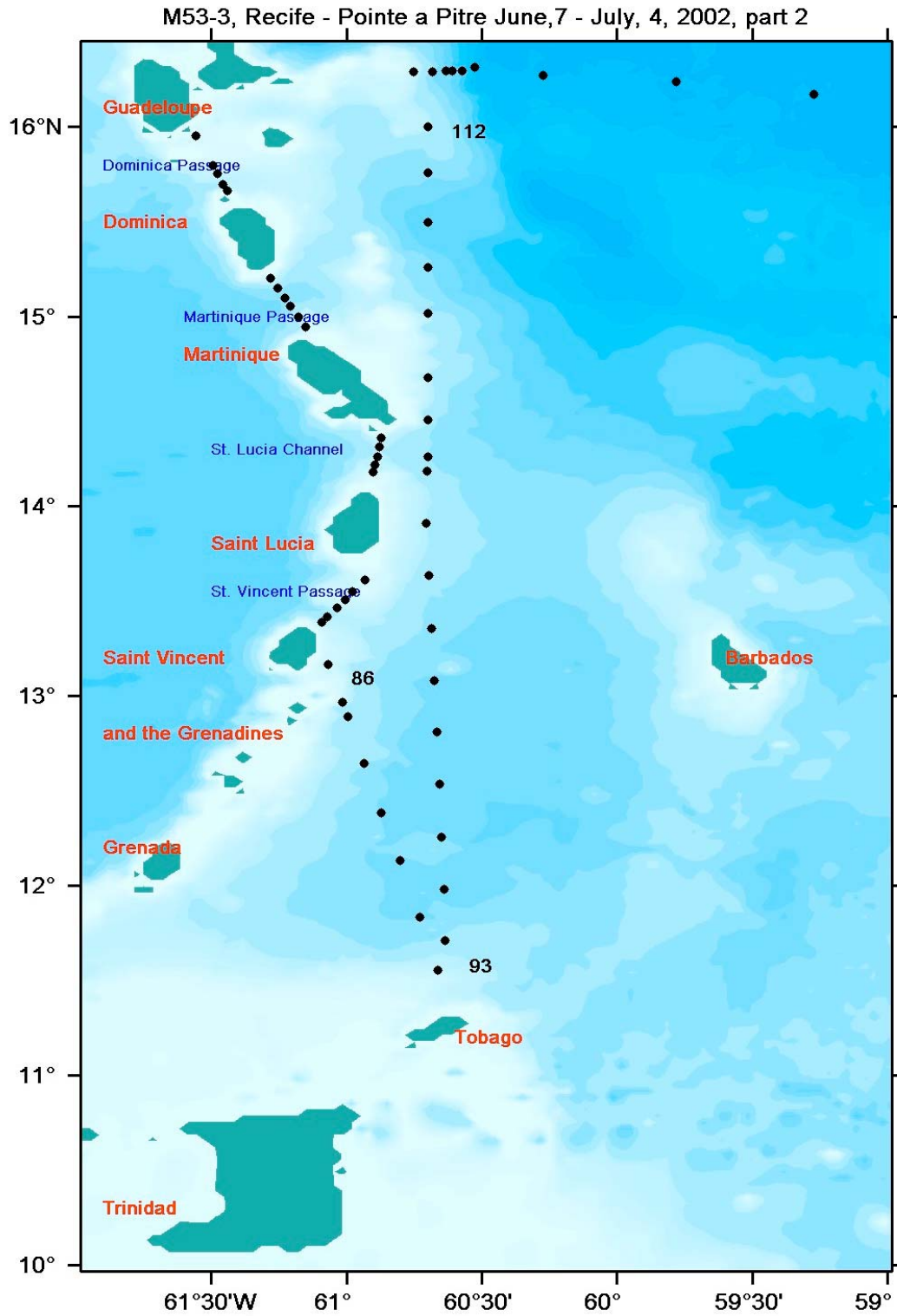


Figure 3-1b

### 3.4 Preliminary results

#### 3.4.1 CTD/Oxygen Measurements and Calibration

During cruise M53/3 two different CTD-O/water sampler systems came into use. Both systems consisted of a 24 bottle Sea-Bird SBE-32 carousel water sampler and a Sea-Bird 911plus CTD sensor. On one system, three bottles were removed and replaced with an IADCP. The CTD at this rosette was additionally supplied with a Beckmann dissolved oxygen sensor. The other rosette retained all 24 bottles and the new SBE 43 dissolved oxygen sensor (Clark polarographic membrane type sensor) was attached to the CTD. Both systems were used alternatively except for the beginning (profile 1 - 26) and end (profile 88 - 111) of the cruise, where only the system with IADCP was brought into operation. At profile 36, the conductivity sensor of the CTD attached to the rosette with IADCP showed irregular high values and was substituted with a sensor of the same type. Two electrical reversing pressure and four temperature sensors were attached to one rosette (21 bottles) and two reversing thermometers to the other (24 bottles). Within the accuracy of these thermometers no deviations to the CTD-temperature were found and no further correction to the laboratory calibration was applied.

About five salinity samples for each profile were taken for the calibration of the three conductivity sensors used during the cruise. The samples were analysed by means of a Guildline Autosol salinometer. Almost no temporal drift of the salinometer within one measurement session could be detected, the standard deviation of the substandard measurements was less than 0.001. The CTD salinity values were corrected using a linear correlation of the deviation with pressure, temperature, conductivity and time. This resulted in an rms-error between CTD and sample values of 0.0024 (0.0016), 0.0028 (0.0023) and 0.0023 (0.0017) for all (below 1000m) samples respectively.

Oxygen samples were measured using a SIS dissolved oxygen analyzer. Roughly ten samples were taken for each profile plus one to two double samples, giving a reproducibility of 0.037 ml/l. The two oxygen sensors attached to the CTDs were calibrated by means of the bottle data taking into account a temporal drift as well as a pressure dependent offset. The rms-error is 0.054 (0.048) ml/l for the Beckmann and 0.045 (0.038) ml/l for the SBE sensor for all (below 1000m) samples. Although the Sea-Bird calibration for the oxygen sensor resulted in much too low values in the deep water range, this could be compensated by fitting new calibration coefficients. An advantage of the new oxygen sensor type seems to be that typical small scale fluctuations (appr. 0.02 ml/l) in the oxygen profiles measured by means of the Beckmann sensor did not show up using the SBE device.

#### 3.4.1b Thermosalinograph Measurements and Calibration

Data from the ship's thermosalinograph has been recorded during the cruise M53/3. Temperature and salinity have been calibrated using the CTD values from 6 m depth. This correction includes a linear correlation of the deviation with time, temperature and, for salinity, also with conductivity. The standard deviations between CTD and thermosalinograph measurements are 0.0046°C for temperature and 0.014 for salinity.

### 3.4.2 Chlorofluorocarbon (CFC) Measurements and Calibration

About 1100 water samples have been analysed for the CFC components CFC-11 and CFC-12. All analysis have been done on board with the Bremen GC/ECD system. The absolute calibration was carried out using a gas standard, which has been recalibrated against the other Kiel and Bremen standards after the cruise. The blank level of the gas standard and the water samples was smaller than 0.002pmol/kg. 5% of the samples were measured twice. The reproducibility was 0.6% for CFC-11, and 0.5% for CFC-12. For CFC-11 concentrations smaller than 0.04pmol/kg and CFC-12 values smaller than 0.025pmol/kg the reproducibility was 0.0005pmol/kg (CFC-11) and 0.0003pmol/kg (CFC-12). After CTD station 65, the reproducibility for CFC-11 concentrations smaller than 0.2pmol/kg and CFC-12 values smaller than 0.4 pmol/kg, the reproducibility increased to 0.002pmol/kg for CFC-11 and 0.004pmol/kg for CFC-12. The deterioration of the reproducibility was caused by the dense station spacing, which allowed only sporadic calibration measurements. The precision for all data was 0.3% for CFC-11 and 0.2% for CFC-12, for values smaller than 0.04pmol/kg (CFC-11) and 0.025pmol/kg (CFC-12), the precision was 0.00015pmol/kg.

### 3.4.3 Direct Current Meter Measurements with VM ADCP / LADCP

#### VMADCP

Two RD Instruments vessel mounted ADCPs were continuously operating during the cruise. One was a 75 kHz phased array Ocean Surveyor installed into the hull of the ship. The other was a new 38 kHz Ocean Surveyor that has been installed into the sea chest at the beginning of the previous leg (M53/2). Both instruments worked flawless throughout the entire cruise. The 75 kHz ADCP is capable of sampling the water column to a depth of up to 700 m while the 38 kHz instrument has a range of up to 1600 m but requires larger depth cells. Therefore a depth cell size of 8 m was chosen for the 75 kHz instrument to get high resolution data of the upper water column. The 38 kHz ADCP was optimized for range with a depth cell size of 32 m. The full range of the ADCPs was only reached in calm conditions while the data quality was reduced in rough sea. Generally good data were acquired in the upper 1200 m during most of the time. Both instruments were sampling at the fastest rate of about 2.3 s for the 75 kHz ADCP and 2.8 s for the 38 kHz ADCP. The temperature sensor of the 75 kHz ADCP was not working properly and was therefore disabled. The speed of sound necessary for the velocity calculation was entered manually for this instrument.

Navigation and heading (GPS, Ashtech) information were recorded together with the velocities through two serial interfaces of the data acquisition computer. Both ADCPs used the syncro version of the Fiber Optic Compass (FOG) heading connected directly to the chassis of the ADCP to transform the measured velocities into earth coordinates although it has been found on an earlier cruise (M47/1) that the FOG has a heading dependent error. Due to this error the data were corrected by substituting the syncro-FOG heading values of each single ping with heading values from the Ashtech system. In general the Ashtech data coverage was very good except for a few short periods. For these periods digital FOG heading data were used for the heading correction. A comparison between the Ocean Surveyor and the lowered ADCP data obtained while on station is shown in Fig. 3- 2.

The misalignment angle of the 75 kHz Ocean Surveyor had already been determined on the previous leg and did not change from its value of 0.84° as the instruments is fixed into the hull of the ship. The 38 kHz instrument in the sea chest was newly installed at the beginning of the cruise due to jumps of the misalignment angle on the previous leg. During most of the

cruise the instrument was now stable with a misalignment angle of  $-2.1^\circ$ , but again showed a small jump of  $0.5^\circ$  near the end of the cruise.

**LADCP**

A narrow-band ADCP (S/N 301 from the Institut für Meereskunde Kiel) was attached to one of the two CTD-rosettes that were in use to obtain full depth velocity profiles at hydrographic stations. The lowered ADCP was used at stations where the bottom was out of the range of the shipboard ADCP except when the cast was below 5000 m, the limit of its pressure case. In total 72 good LADCP profiles were collected.

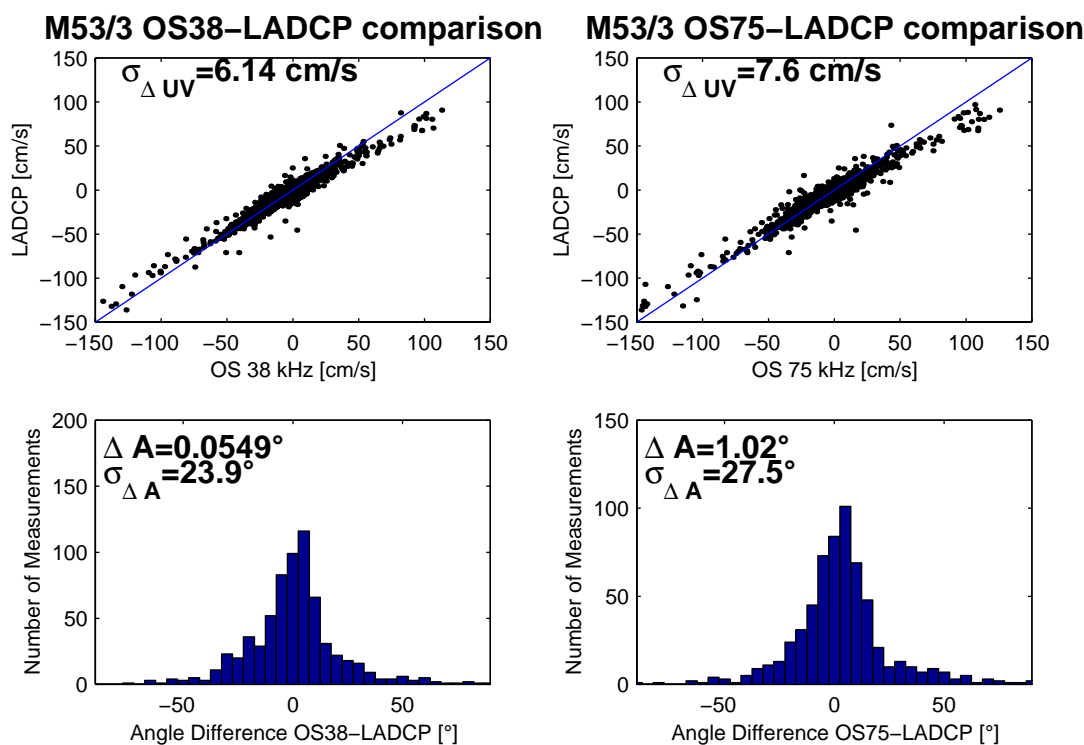


Figure 3-2: Comparison between magnitude and direction of the vessel mounted ADCP and the lowered ADCP for both the 38 kHz Ocean Surveyor (left panel) and the 75 kHz Ocean Surveyor (right panel).

### 3.4.4 The warm limb of the Meridional Overturning Circulation

The upper part of the thermohaline circulation in the tropical Atlantic consists of warm water from the South Atlantic. It enters the Northern Atlantic mainly in the North Brazil Undercurrent (NBUc) and the South Equatorial Current (SEC). Both currents combine between 35°W and 40°W and create the North Brazil Current (NBC), flowing along the Brazilian coast (Schott et al., 1995; 1998). Part of the NBC joins the zonal equatorial flows. North of the retroflexion zone of the NBC-NECC (North Equatorial Counter Current) the northward transport of warm water mainly occurs in eddies (Didden and Schott, 1993), the transport is therefore difficult to assess.

The NBC transport is much higher than the net interhemispheric water exchange. Part of the NBC flows back into the South Atlantic through the equatorial current system. Owing to significant variability in the transport and divergences in the wind field, the net exchange cannot be measured easily. Ultimately, the main part of the southern hemispheric water which remains in the North Atlantic is thought to flow into the Caribbean. Part of the water, especially the intermediate water flows east of the Caribbean to the north and both branches join the Florida Current.

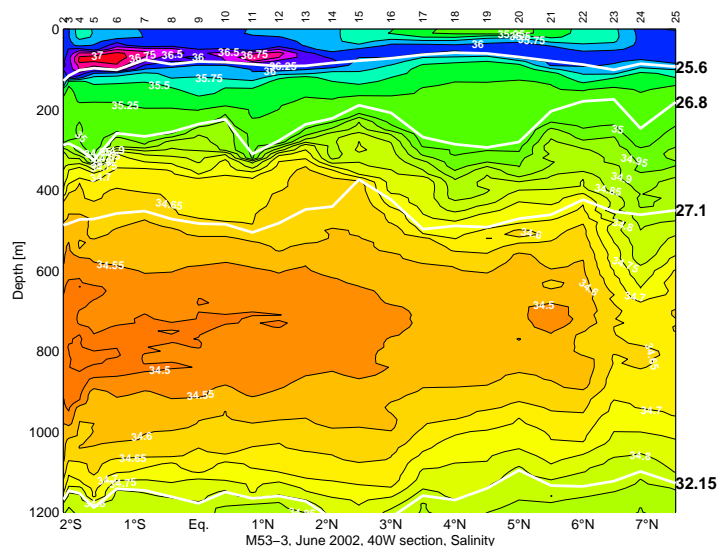


Figure 3-3 Salinity distribution in the upper 1200m along the 40°W section

### **The water masses**

The upper and intermediate water masses in the tropical Atlantic are depicted in the salinity distribution along 40°W (Fig. 3-3). The Salinity Maximum Water (SMW) between 50 and 100m depth is embedded in the Tropical Surface Water (TSW) reaching from the surface to the  $\sigma = 25.6$  isopycnal. This isopycnal represents the 20°C isotherm, which is frequently used to define the lower limit of the TSW. The salinity maximum is strongest in the NBC off Brazil and around 1°N in the SEC (Figs 3-3, 3-4). The SMW is subducted in the subtropical South Atlantic where it gained the high salinity values at the surface. Below the TSW, the South Atlantic Central Water (SACW) is found, its lower limit is the  $\sigma = 27.1$  isopycnal. The  $\sigma = 26.8$  separates the zone with weak vertical gradients from the denser part with strong vertical gradients. The profiles in the northern part of the section show some contribution of North Atlantic central Water (NACW), especially below  $\sigma=26.8$ . The salinity minimum centered at 800m depth characterizes the Antarctic Intermediate Water (AAIW).

### **Velocity field**

The near surface current system (Figure 3-4) shows the North Brazil Current (NBC) off Brazil together with the South Equatorial Current (SEC), both flowing northwestward mainly parallel to the coast. In the NBC, the velocities exceeded 1m/s, and the transport of both currents was 60 Sv. The SEC is separated in a southern and a northern part at the Equator by the Equatorial Undercurrent (EUC) flowing eastwards with 30 Sv and reaching into the surface layer. North of 4°N, one expects to find an eastward flowing North Equatorial Counter Current (NECC). The NECC reaches its maximum eastward transport in August, and weaker or even westward flow is sometimes found in late boreal winter. Surprisingly, the flow was still to the west (9.4Sv), and the low salinity reflects water of eastern Atlantic origin (Figure 3-3).

Below the surface the eastward flowing North Equatorial Undercurrent (NEUC), ranges from 4°N to 6°N. The velocity core of the NEUC was located at 150m depth with velocities exceeding 50cm/s and the eastward flow (28 Sv) was present down to depths of about 800m. The core of the westward flowing Equatorial Intermediate Current (EIC) is found in 600m depth at the equator, bounded in the north at 1°30'N by the eastward flowing North Intermediate Counter Current (NICC). The EIC transports 38 Sv, the NICC about 16 Sv. A weak South Intermediate Counter Current (SICC) is observed south of 1°40' S, reaching below 1200m. The AAIW flows westward with the downward extension of the NBC and with the EIC, and part of it recirculates north of 5°N and flows eastward with the NICC between 5°N and 6°N.

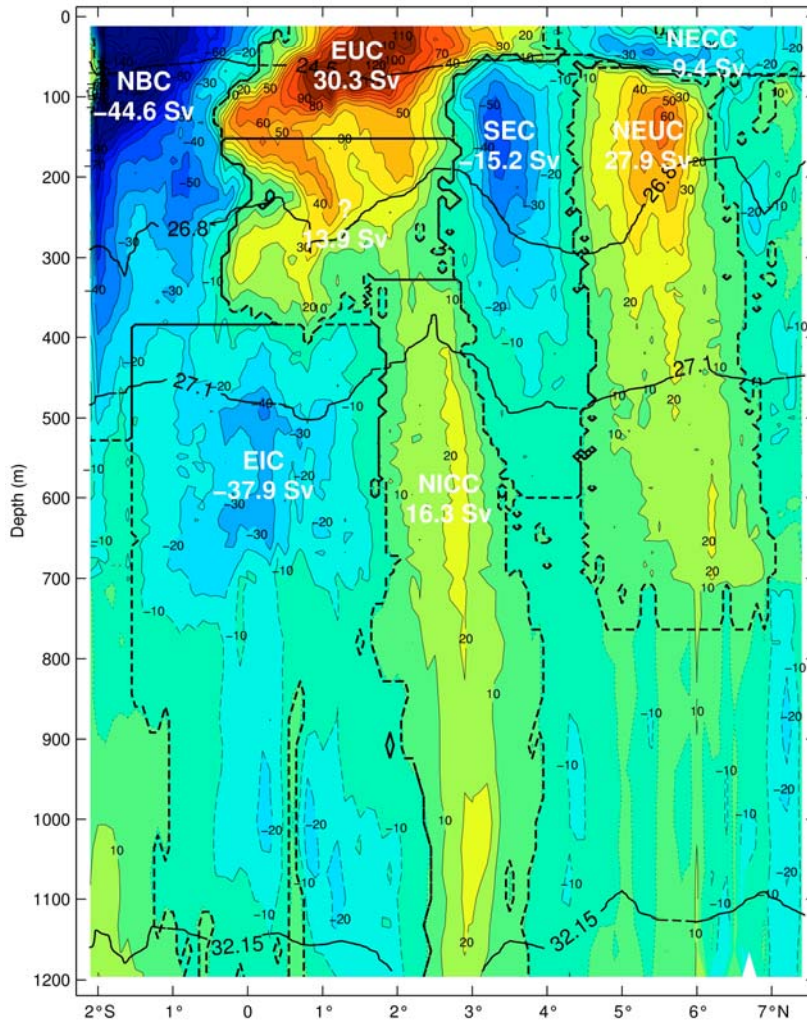


Figure 3-4. Zonal velocity distribution along 40°W, measured with the 38.5kHz Ocean Surveyor

### 3.4.5 Contribution of southern hemispheric water

To determine the fraction of South Atlantic water in the data of the M53-2 and M53-3 cruises, isopycnal mixing was assumed and the fraction was calculated from the distribution of potential temperature and salinity. The source water masses are SACW (South Atlantic Central Water) and NACW (North Atlantic Central Water). SACW was defined at 10°S off Brazil (cruise S-171), similar to the definition from Poole and Tomczak (1999). The deep part of the NACW was defined at 24°N (WOCE section A05, 1992), for lower densities S-152 measurements at 16°N, 57°W (S-152 cruise) were used (Figure 3-5). The 24°N data were used because the S-152 salinities were lower than the definition of Poole and Tomczak. In the density layers of the SMW, the influence of a source water mass from the eastern equatorial Atlantic was noted (Figure 3-6), and the characteristic of this water (named ESW) was defined from measurements at 2°N, 23°W (cruise M47). The density layers chosen were a) Salinity maximum water SMW ( $25.5 < \sigma < 26.3$ ); b) upper central water ( $26.3 < \sigma < 26.8$ ), c) lower central water ( $26.8 < \sigma < 27.1$ ), and d) intermediate water ( $27.1 < \sigma < 27.4$ ). Densities shallower than  $\sigma = 25.5$  could not be included in the calculation, since they outcrop in the research region. Thus the SMW layer only includes the densities below the salinity maximum.

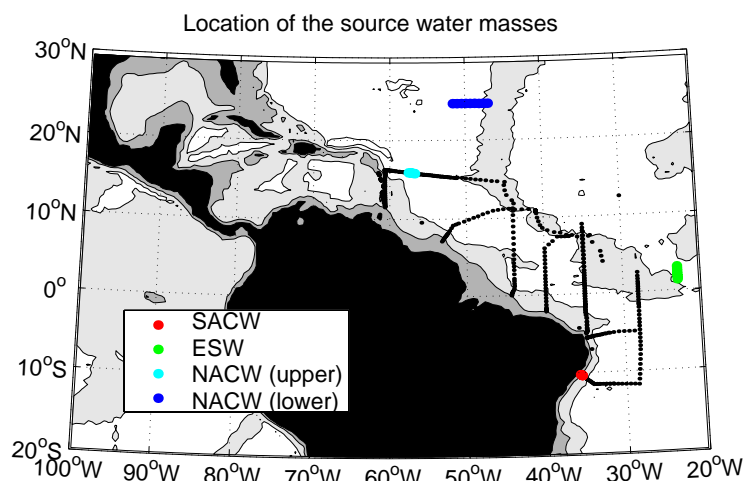


Figure 3-5 Location of the source water masses for the T-S analysis

In November 2000, for the Salinity maximum water (Fig 3-7a) the contribution of southern hemispheric water at the 16°N section is lower than 20%. In the upper central water (Fig.3-7b), up to 50% are found on some location, but in general, the fraction is lower than 20%. For both water masses, the difference between the 7°30N section and the 16°N section is striking, the fraction of South Atlantic water decreases about 50-70% to lower than 20%, indicating a

possible transport of the southern hemispheric water into the Caribbean trough the passages between Guadeloupe and South America.

For the lower central water, however, the contribution from the South Atlantic at 16°N are mostly between 20-40% (Fig. 3-7c), and in the intermediate water range about 50-70% are from the South Atlantic (Fig. 3-7d). This is the northward flowing Antarctic Intermediate Water (AAIW), which carries a salinity minimum from its source region in the circumpolar current into the subtropical North Atlantic. For both water masses, the inflow into the Caribbean is more restricted by the topography, by limited depths of the passages and limited area of the throughflow. At the 35°W section and further east and south, the southern hemispheric water contributes more than 70-80% .

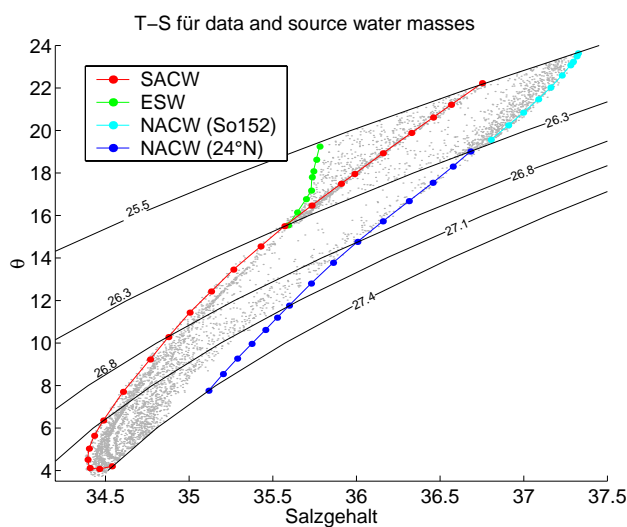


Figure 3-6 T-S diagram for the data and source water masses. The uppermost layer encompasses the lower part of the salinity maximum water.

The METEOR M53 data (Fig. 3-8) were taken in boreal summer. It seems, that for the upper and lower central water, the fraction of southern hemispheric water along 16°N is higher in autumn than in spring (Figure 3-8). During the M53-3 cruise, measurements in and east of the passages south of Guadeloupe were taken. The contribution of South Atlantic water is highest in the southern passages, 40-50% for the lighter water masses, and 50-70% for the lower central water and the intermediate water. The inflow of intermediate water into the Caribbean is however negligible, since the passages are too shallow.

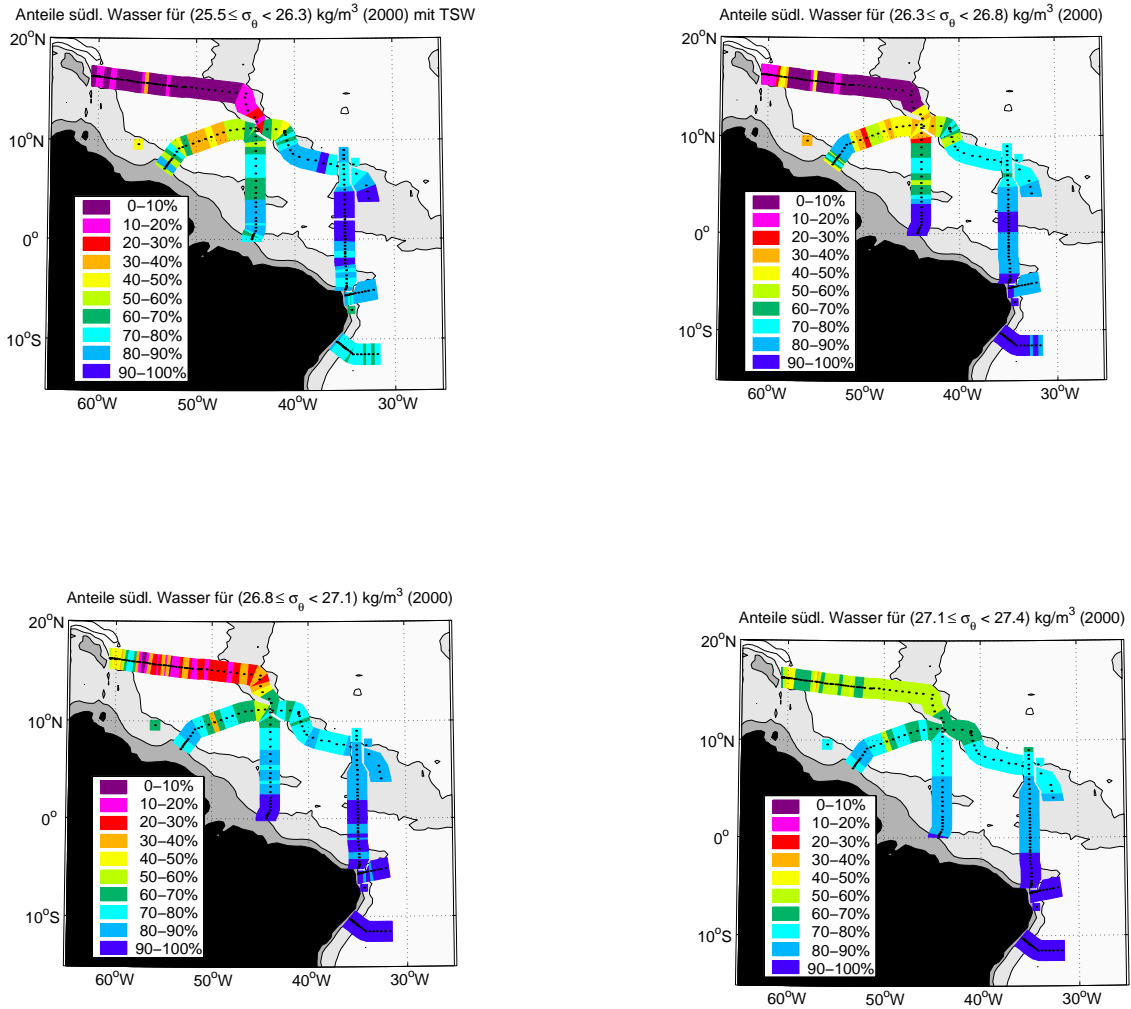


Figure 3-7 Fraction (in percent) of water from the South Atlantic, November 2000 .a) salinity maximum water, b) upper central water, c) lower central water; d) Intermediate water

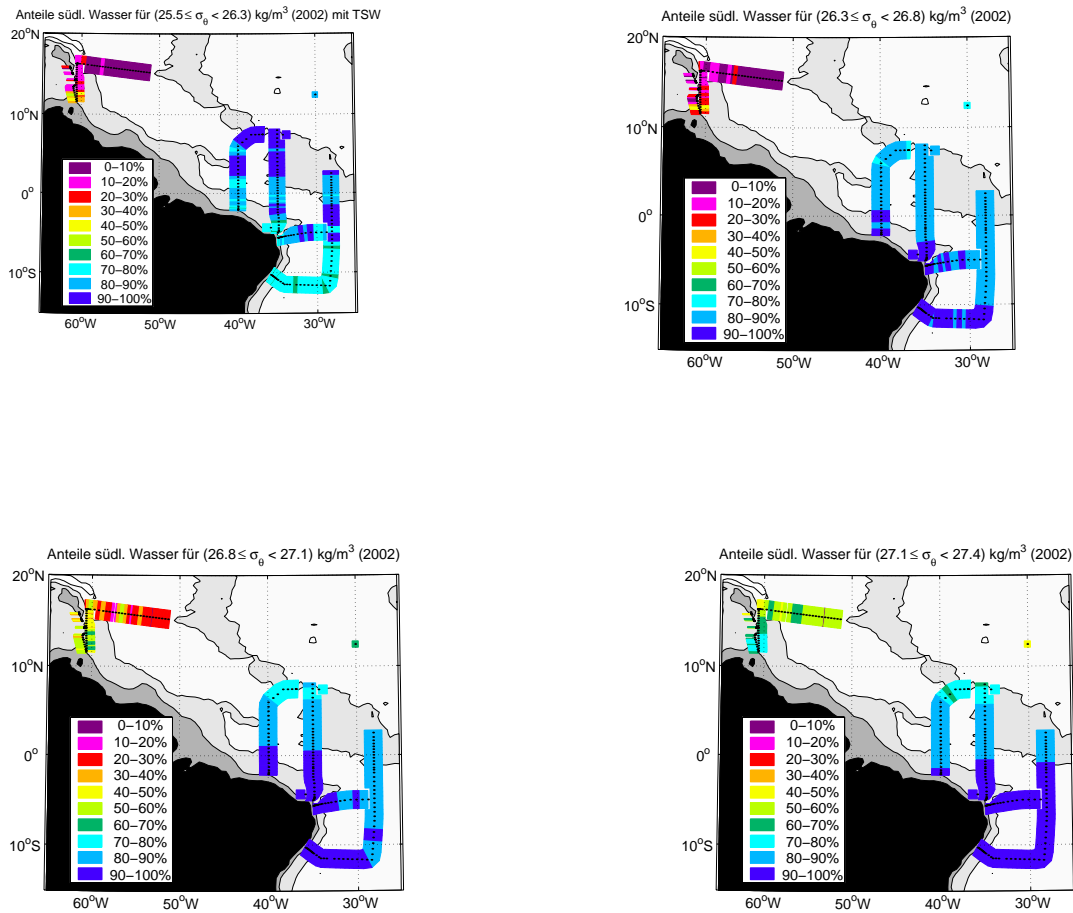
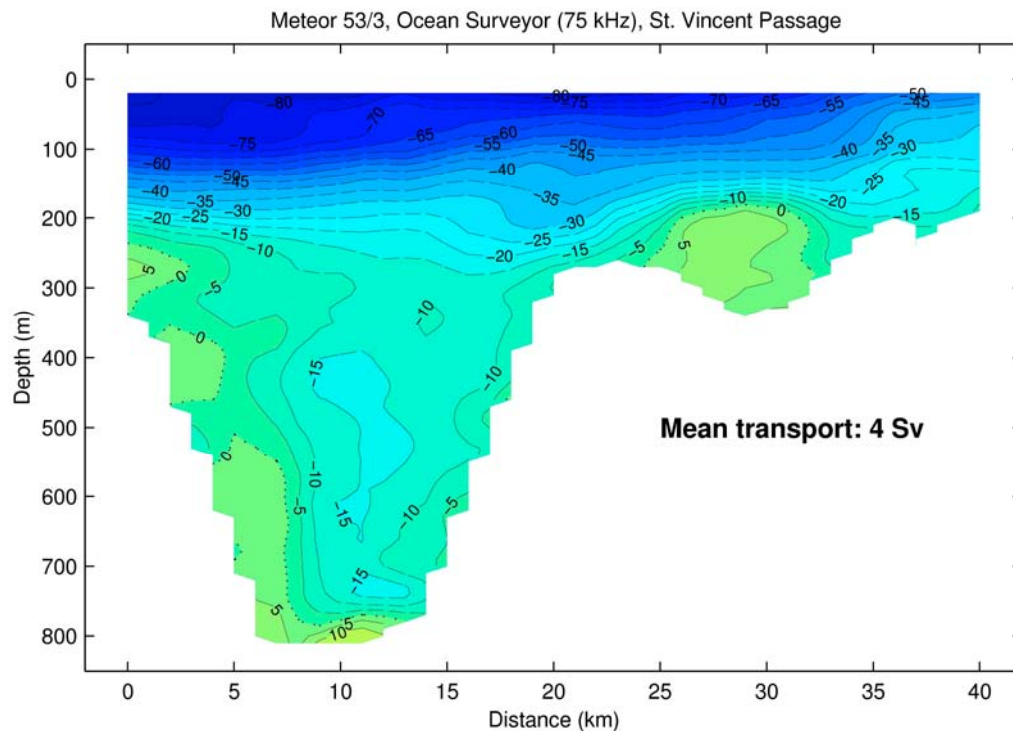


Figure 3-8 Fraction (in percent) of water from the South Atlantic, M53-2 and M53-3 data. a) salinity maximum water, b) upper central water, c) lower central water; d) Intermediate water

### 3.4.6. Velocity measurements in the passages south of Guadeloupe

The vessel mounted 75kHz ADCP was used to measure the velocity field in the passages. 5 repeats have been carried out in order to remove the influence of the tides. The highest transport in the passages was found in the St. Vincent passage with a mean of 4 Sv (Fig.3-9). On all sections, the net transport was into the Caribbean, the highest velocities were observed in the upper 200m. That means that the inflow of the tropical surface water TSW was highest, with decreasing transports with depth. In total, the inflow into the Caribbean during the M53-3 campaign was about 8 Sv.

Figure 3-9 Mean zonal velocity field from 5 repeats through the St. Vincent Passage. Negative: westward flow, i.e. into the Caribbean.



### 3.4.7 The cold limb of the meridional overturning circulation MOC

In the Atlantic, the cold limb of the Meridional Overturning Circulation (MOC) consists mainly of North Atlantic Deep Water (NADW). One of the major components is water formed in the Labrador Sea by convection, the Labrador Sea Water (LSW). Lighter modes are called upper LSW (uLSW), and uLSW might be formed each winter, albeit with different intensities and on different locations (Pickart et al., 1992; Stramma et al., 2003). The denser modes (LSW) are only formed sporadically depending on the climatic conditions and the stratification in the source region (Lazier et al., 2002). ULSW and LSW form the upper limb of the NADW (upper NADW). The middle and lower NADW consists mainly of overflow water, spilling over the sills between Iceland and Scotland (Iceland Scotland Overflow Water, ISOW) and over the Denmark Strait (Denmark Strait Overflow Water, DSOW). The DSOW part is called lower NADW.

The NADW water masses mainly spread south with the Deep Western Boundary Current. In all DWBC sections made since the early 1980s, a CFC maximum was observed in the upper NADW at about 1600-1800m depth, characterizing uLSW (e.g. Weiss et al., 1985; Rhein et al., 1995; Andrie et al., 2002). The CFCs have been introduced into this water mass by convection. The temporal atmospheric CFC increase is reflected in the temporal CFC increase in this water mass in the DWBC, although modified by mixing and recirculation. This transient CFC signal have been used frequently to estimate transit times (and mean spreading velocities) of the DWBC from the source region to the subtropical and tropical Atlantic (Andrie et al., 2002; Fine et al., 2002).

Since convection activities in the 1970s and 1980s were mainly restricted to the uLSW range, the LSW exhibits no special CFC signal in the tropical Atlantic, but the arrival of CFC enriched LSW, which has been formed between 1988 and 1994 is expected at the equator in the next years (Stramma and Rhein, 2001). A second CFC core around 3800m depth in the lower NADW observed in the DWBC is a feature of the DSOW (Rhein, 1994).

When reaching the equator, both, the upper and the lower CFC core bifurcate, with some of the NADW spreading eastward, and the other part continues with the DWBC along the continental slope of Brazil. The spreading towards the east occur with deep jets, which have been observed with SOFAR floats, deployed at 1800m depth (Richardson and Fratantoni, 1999).

### **The deep water masses along 40°W**

The deep water masses along 40°W consists of several components of the North Atlantic Deep Water, NADW, which are transported towards the equator mainly in a Deep Western Boundary Current (Fig. 3-10). The shallow part, bounded by  $\sigma_{\theta} = 34.42$  and  $34.755$  originates in the Labrador Sea and is formed by convection there. The isopycnal  $\sigma_{\theta} = 34.750$  separates the lighter modes of LSW, the uLSW (upper LSW) which were formed each winter, from the denser modes, the cLSW (classical LSW, henceforth called LSW). The formation of LSW is subject to significant interannual variability. Intense formation took place in the early 1970s and in the 1988-1994. During convection, the uLSW and LSW get tagged with atmospheric trace gases like the CFC component CFC-11 (Fig. 3-10). In former years, only the uLSW carried a CFC maxima into the tropical Atlantic, here observed in about 1600-1800m depth.

The deepest CFC maximum at 3600m-3800m depth extends from the Brazilian continental shelf to about 6°N, with a southern core at 1°30'S at the bottom and a northern core between 1°N and 2°N. This water mass originates north of Iceland and is also characterized by a CFC maximum. When overflowing the Denmark Strait between Greenland and Iceland, the DSOW (Denmark Strait Overflow Water), transport increases and the water mass characteristics were altered, but the CFC – maximum remains. The DSOW is bounded by the isopycnals  $\sigma_{\theta} = 45.83$  and  $45.90$ . At 40°W, the southern DSOW core is part of the DWBC, flowing eastward with a speed around 10cm/s (Figure 3-11). The northern core also flows eastward. The water between 2500 and 3200m in the CFC-minimum zone consists mainly of deep water flowing into the Western Atlantic through the Charlie Gibbs Fracture Zone at 53°N (GFZW, Gibbs Fracture Zone Water).

The CFC-Minimum at the bottom represents the Antarctic Bottom Water (AABW). Constrained by the Mid Atlantic Ridge, the AABW flows from the southern hemisphere into the western North Atlantic through the equatorial channel at 35°W between 1°30'S and 0°50'N. In the tropical Atlantic, the rising topography blocks the flow of AABW south of 1°30'N. The AABW is defined having densities higher than  $\sigma_{\theta} = 45.90$ . At 40°W, the coldest and densest AABW is found at 2°N, another core is located at 5°N (Fig. 3-10).

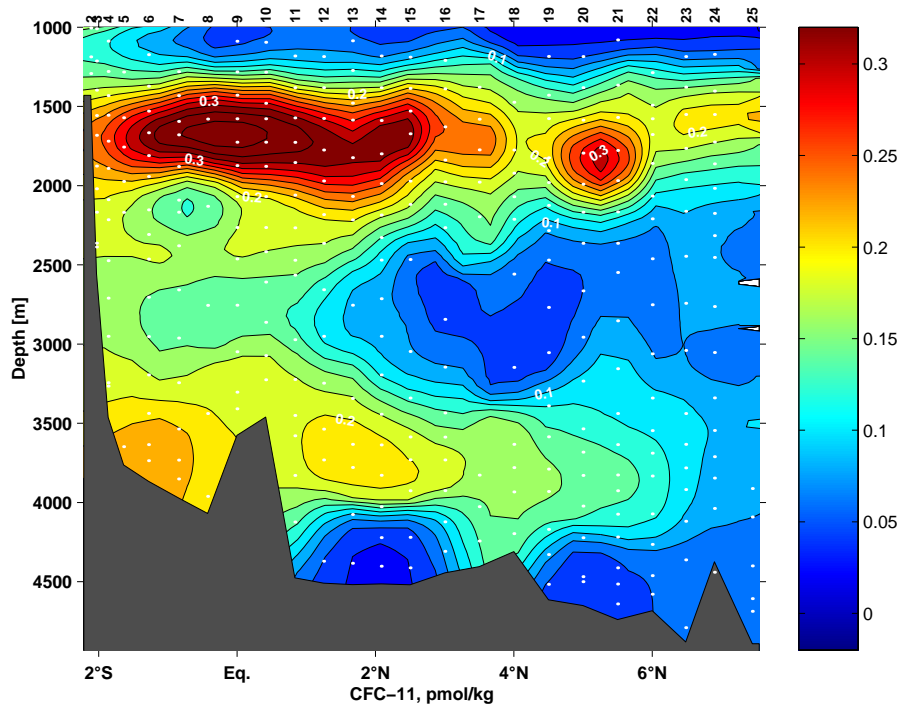


Figure 3-10 CFC-11 distribution (pmol/kg) along 40°W, Meteor cruise M53-3

A conspicuous feature occurred in the CFC profiles at 40°W in the region south of 1°15'N, i.e. in the DWBC. From 2°S to 1°15'N, a coherent second CFC-11 maximum occurred at sig1500=34.74, the density of LSW. The CFC minimum had a density of sig1500= 34.72. The uLSW max was located at sig1500=34.65. No sign of the 2<sup>nd</sup> max was found north of 1°15'N, although a strong uLSW signal comparable to the one in the DWBC was found between 2°N-3°N and 5°N-6°N.

At first we interpreted the 2<sup>nd</sup> max in the DWBC as the arrival of the 1988-1994 LSW at the equator. If this assumption holds, then one expects to find the elevated CFC values associated with a salinity decrease. The salinity profiles do show a dent in the profiles of about -0.005, but the salinity minimum was at sig1500=34.72, parallel to the CFC minimum. The 2<sup>nd</sup> CFC max at sig1500=34.74 was below the salinity minimum and thus not associated with a salinity signal. Moreover, the CFC concentrations in the uLSW max and the 2<sup>nd</sup> maximum increased in the 8 years since 1994 by 140% and 160%, respectively, but only by 80% in the CFC minimum. Outside the LSW, the increase is roughly 100%.

The zonal velocity distribution is mainly eastward in the DWBC range (Fig. 3-11), but predominantly westward in the CFC minimum zone at about 2000m depth. These features lead to the conclusion, the the salinity and CFC minimum was advected by the deep equatorial currents from the east, separating the two eastward flowing bands of high CFC water.

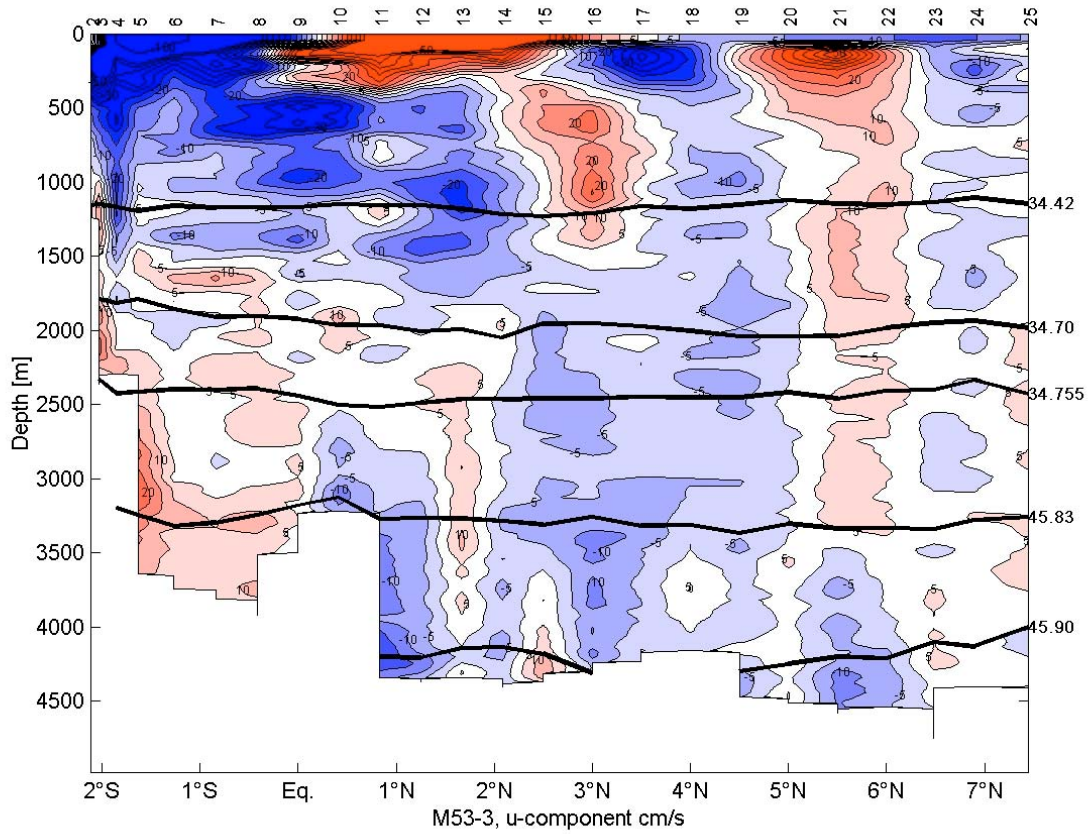


Figure 3-11 Zonal velocity field measured with LADCP along 40°W, Meteor cruise M53-3. Red: eastward flow, blue: westward flow

### 3.4.8 CFC-derived ages of NADW in the tropical Atlantic

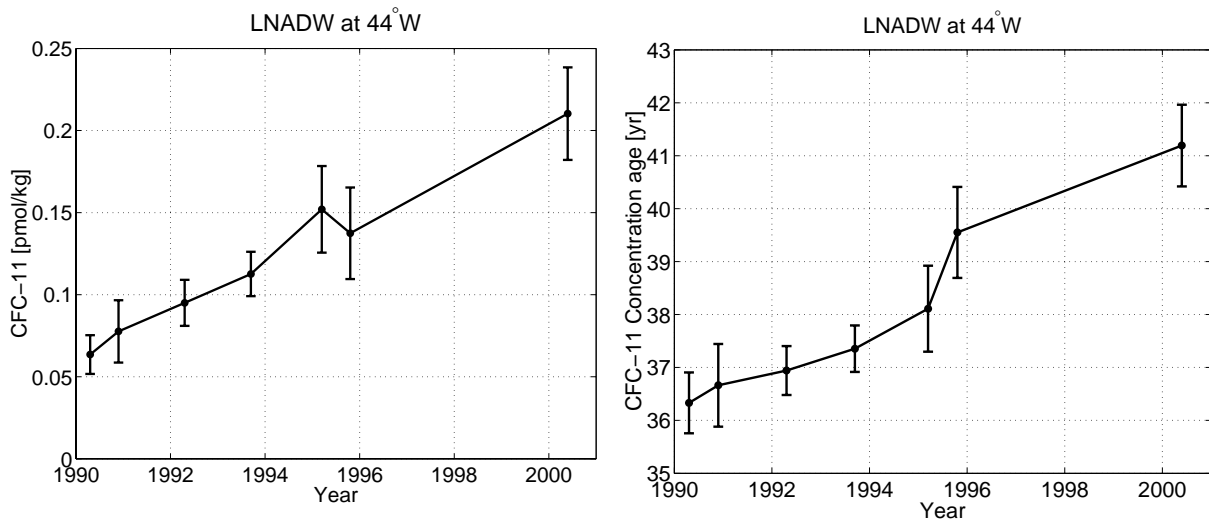


Fig.3-12: CFC-11 concentration (left) and CFC-11 concentration age (right) in the LNADW density range for the repeated sections at 44°W in the tropical Atlantic

### a) Concentration Age

The concept of 'ages' can be used to interpret the transient CFC-signal in the ocean interior. The age of a water mass is the time elapsed since its formation, i.e. when the water was last exposed to the atmosphere. The time of water mass formation according to the concept of concentration age is determined as the year when the measured oceanic CFC-concentration equals the solubility equilibrium of the atmospheric CFC-mixing ratio (Doney and Bullister, 1992). Normally, however, the newly formed water is undersaturated with respect to CFCs because of the entrainment of older water during the formation process. In the Labrador Sea, for example, the concentration age of Labrador Sea Water (LSW) is about 10 years. This can be taken into consideration by subtracting the 'relic' age from the calculated concentration age (Fine et al., 2002).

In the tropical Atlantic, mean core concentrations of CFCs are calculated for the density ranges of UNADW, LSW and LNADW at the specific sections. Fig. 3-12 shows the results for the repeated measurements at 44°W within the LNADW layer. The CFC-11 concentration shows an increase from 0.05 to 0.2 pmol/kg over the observational period from 1990 to 2001. The CFC-concentration age is not exactly constant in time. The change from 36 to 41 years, however, is comparatively low. This change may be due to variability of NADW transport, but it is also a consequence of the nonlinear behaviour of the concentration age under mixing processes in the ocean interior.

### b) Age Spectra in the Tropical Atlantic

The concept of age spectra (Hall and Plumb, 1994) considers both the change of the atmospheric CFC-content and the transport and mixing processes in the ocean. Therefore a water parcel is considered as a composition of infinitesimal fluid elements with different ages and CFC-concentrations. The age spectra describe the distribution density of ages within the water parcel. For a 1-dimensional, steady state circulation an analytical solution for the age spectra exists. This analytical expression fulfills the advection-diffusion equation and depends on the velocity  $u$  and diffusivity  $k$  of the flow. Additionally, the mixing of NADW with 'old' water free of CFCs is accounted for by a dilution factor  $f$  ( $0 < f < 1$ ). The parameters  $u$ ,  $k$ , and  $f$  are fitted by minimizing the deviation between the CFC-concentrations computed by the age spectra and the measured values. In accordance to the 1-dimensional solution,  $u$  and  $k$  are the same for each water mass at all sections. The fraction  $f$  is varying from section to section, but only solution with downstream decreasing values of  $f$  are acceptable.

A range of values has been determined for the parameters  $u$ ,  $k$  and  $f$ , yielding the observed evolution of CFC-concentrations. It is not possible to give a reliable estimation of the diffusivity  $k$ , possible values range from 100 to 10000 m<sup>2</sup>/s. The velocity, however, is restricted to a relatively small interval from 1.5 to 2.0 cm/s. These values are comparable to earlier results based on the interpretation of CFC-data in the tropical Atlantic (Andrié et al., 2002). The fraction  $f$  of pure NADW shows the required southward decrease, indicating the mixing of NADW with water from Antarctica (Fig.3-13).

The signal of enhanced LSW formation, resulting from intense deep convection from 1972 to 1976 and 1988 to 1994 in the Labrador Sea, should be reflected by a strong increase of CFCs in the LSW-range in the tropical Atlantic (Freudenthal and Andrié, 2002). Near the equator, however, this signal is overlaid by the variability of the equatorial current system. Transient Equatorial Deep Jets export NADW into the eastern Atlantic, leading to a sporadic decrease of CFC-content in the Deep Western Boundary Current.

For the northernmost section at 16°N, where the signal of LSW is expected to be strongest, only two realisations have been performed so far in 2000 and 2002. Assuming a mean current speed of about 1.5 cm/s, the LSW-signal from the 1970s has already passed the 16°N section,

whereas the signal from the late 1980s will arrive not before 2005. Repeated measurements at this section therefore provide a good means to test the estimation of spreading velocities for NADW.

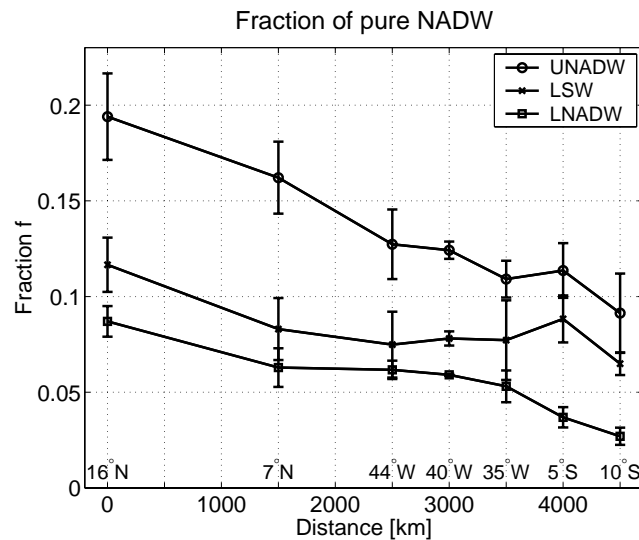


Fig.3-13: Fraction  $f$  of pure NADW for UNADW, LSW and LNADW. The belonging values for velocity and diffusivity are  $k = 1000 \text{ m}^2/\text{s}$  and  $u = 1.5 \text{ cm/s}$  for UNADW and LSW and  $2.0 \text{ cm/s}$  for LNADW.

### 3.4.9 Arrival of newly ventilated LSW at 16°N

Historical data are sparse at 16°N and CFCs have been measured at that location only in 2000 and 2002. Although the mean velocity derived from age spectra is too low for the 1988-94 LSW to have arrived at 16°N, there are several indications that the LSW formed in 1988-1994 might have passed that location already. Compared to 1989, the uLSW and LSW cooled and freshened in 2000 by about 0.01, and the data from 2002 were again fresher by 0.007. The cooling and freshening was restricted to the boundary region. Fig 14 shows the differences in the CFC concentrations between the Sonne cruise So-152 in December 2000 and the Meteor cruise M53-3 in June 2002. The greatest increase was observed between 1600 and 2400m depth near the western boundary west of 60°W. This increase might be caused by the arrival of newly ventilated LSW, which was formed in the central Labrador Sea in 1988-1994.

The moored temperature and salinity time series of the MOVE/GAGE array, however, show a variability in 2100m depth (LSW) in the order of  $\pm 0.01$  in salinity, making the observed salinity decrease from shipboard observations ambiguous. But a trend to decreasing salinities and to cooling cannot be excluded from the two year time series (U.Send, T.Kanzpw, pers.comm.). For densities greater than  $\sigma_{1500} = 34.63$ , the CFC-11 increase was strongest west of 60°W, i.e. in the DWBC. The CFC maximum was 0.95 pmol/kg, slightly lower than the 1.1-1.3 pmol/kg at 26.5°N in 1996, the arrival year of the 88-94 LSW at that location. In the interior, at several locations, CFC-11 decrease to -0.3 pmol/kg or increase were found for

densities lighter than 34.65, due to horizontal shifts in the recirculation or interior recirculation, respectively.

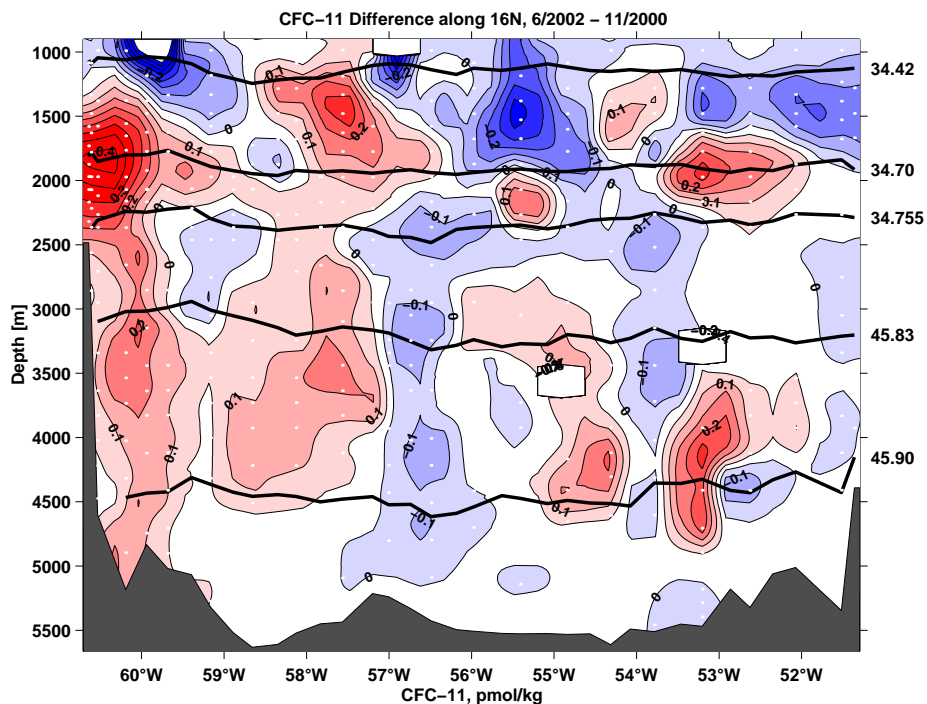


Figure 3-14: CFC-11 differences (pmol/kg) between June 2002 and December 2000 along 16°N

### 3.4.10 Mooring Activities

On previous cruise, there were indications from shipboard measurements that some lower NADW might leave the western Atlantic basin through passages south of the well known Vema Fracture Zone at 11°N. During M53-3 we deployed 2 deep moorings in the 7°30'N passage in order to estimate this throughflow. The positions of the moorings can be viewed in Figure 3-1. Both moorings were recovered successfully on SONNE cruise S-171 in June 2003.

#### Moored CFC sampler

During the M53-3 cruise the Bremen CFC sampler (Fig. 3-15) was tested for the first time by putting the device into 2000m for several hours. The moored sampler was developed in Bremen by modifying a commercially available nutrient sampler for the measurements of CFCs in deep water. The main purpose is to obtain year long time series of CFC concentrations in deep water. In both tests, the sampler showed no contamination affecting the

analysis of CFCs .On the third test, problems with the step motor prevented further activities, and the instrument was sent back to the company after the end of the cruise.



*Figure 3-15. The Bremen CFC sampler on Meteor cruise M53-3.*

### **3.5 Ship's Meteorological Station**

FS METEOR left the port of Recife for leg M53/3 in the early morning of June 07 2002. The voyage from Recife to the first point of investigations near 02° South 40° West followed the northern edge of a south Atlantic subtropical high pressure system. Accompanied by some showers the cruise began with southeasterly trade winds of Bft 4 to 5. Winds and showers abated in the afternoon. On June 09 METEOR started a northerly cross section near 02° S along 40° West with light and variable winds at first, then light northwesterly winds, backing easterly to southeasterly with rapidly changing clouds but little shower activity. During the night from June 11 to 12 METEOR reached the southern edge of the ITCZ (Inter Tropical Convergence Zone) and encountered still relatively broken clouds and only few showers. On the next day (June 13) however, a long and intensive shower activity started associated with isolated thunderstorms. Winds were mainly easterly or southeasterly force 2 to 4, within showers force 4 to 6 and gusts 8. From the most northern point of the cross-section along 40° West the cruise headed northeasterly until about 7.30° North 34.18° West on June 16. There METEOR was in area of the ITCZ as well, which extended until about 09° North. The shower activity was heavy, but decreased on the last day. In the night from June 16 to 17 METEOR left the ITCZ with a direct northwesterly course for a longer leg of about 1000 miles. The wind veered to northeast and on the next day the southern flank of a central northatlantic high

was reached. In this trade wind region southeasterly winds of Bft 5 or 6 were encountered. Until the position of 15.18° North and 51.24° West the weather was mainly fair within varying clouds and winds veering easterly about 5 Bft.

The further voyage along the 16<sup>th</sup> degree of latitude until Guadeloupe was influenced by nearly the same cloudiness, temporary slight shower activity and easterly winds about 5 Bft.

During the last part of the voyage from Guadeloupe along and between the lesser Antilles until Tobago the easterly trade winds of Bft 5 or 6 continued. Some local corner and jet-effects occurred in the vicinity of the islands, pushing the wind on to Bft 7.

During the rest of the leg to the north until Guadeloupe METEOR remained on the border of the north Atlantic subtropical high. The weather was mainly settled apart from some showers, which developed from an outer cloudband of the ITCZ. The constant trade winds came from east with 4 to 6 Bft. On July 04 in the morning the 3<sup>rd</sup> leg of the 53th voyage of METEOR ended in the harbour of Point à Pitre.

### 3.6 References

Andrie, C., J.F. Ternon, M.J. Messias, L. Memery, and B. Bourles, Chlorfluoromethanes distributions in the deep equatorial Atlantic during January – March 1993. *Deep-Sea Res. I* 45, 903-930, 1998.

Andrie, C., M.Rhein, C.Freudenthal und O.Plähn, CFC time series in the deep water masses of the tropical Atlantic, 1990-99. *Deep Sea Res I*, 49, 281-304, 2002

Doney, S.C und J. Bullister, A chlorofluorocarbon section section in the eastern North Atlantic, *Deep Sea Res.*, 39:1857-1883, 1992

Fine, R., M. Rhein und C.Andrie, Using a CFC effective age to estimate propagation and storage of climate anomalies in the deep western North Atlantic Ocean. *Geophys. Res. Lett.* 29, No. 24, doi:10.1029/2002GL015618, 2002.

Fischer, J., and F.A. Schott, Seasonal transport variability of the deep western boundary current in the equatorial Atlantic. *J. Geophys. Res.* 102, 27.751-27.769, 1997

Freudenthal, S. und C. Andrié, The arrival of a 'new' Labrador Sea Water signal in the tropical Atlantic in 1996, *Geophys. Res. Lett.*, 29(0), 10.1029/2002GL015062, 2002

Hall, T.M. und R.A. Plumb, Age as a diagnostic of stratospheric transport, *J. Geophys. Res.*, 99, 1059 -1070, 1994

Lazier, J., R. Hendry, A. Clarke, I. Yashayaev, and P. Rhines, Convection and restratification in the Labrador Sea, 1990-2000. *Deep-Sea Res. I*, 49, 1819-1835, 2002

Pickart, R.S., Water mass components of the North Atlantic Deep Western Boundary Current. *Deep-Sea Res. I* 39, 1553-1572, 1992.

Rhein, M., The deep western boundary current: tracers and velocities. *Deep-Sea Res. I* 41, 263-281, 1994.

Rhein, M., L. Stramma, and U. Send, The Atlantic deep western boundary current: water masses and transports near the equator. *J. Geophys. Res.* 100, 2441-2457, 1995

Rhein, M., O. Plähn, R. Bayer, L. Stramma, und M. Arnold, The temporal evolution of the tracer signal in the Deep Western Boundary Current, tropical Atlantic, *J. Geophys. Res.*, 103C,15.869-15.884, 1998

Richardson, P.L., and D.M. Fratantoni, Float trajectories in the deep western boundary current and deep equatorial jets of the tropical Atlantic. *Deep-Sea Res. II*, 46, 305-333, 1999.

Schott, F., M.Dengler, L. P. Brandt, K.Affler, J. Fischer, B. Bourles, Y. Gouriou, R.L. Molinari and M. Rhein, The zonal currents and transports at 35°W in the tropical Atlantic. *Geophys. Res. Lett.*, in press, Jan 2003.

Stramma, L., and M. Rhein, Variability in the Deep Western Boundary Current in the equatorial Atlantic at 44°W. *Geophys. Res. Lett.*, 28, 1623-1626, 2001.

Stramma, L., D. Kieke, M. Rhein, F. Schott, I. Yashayaev, and K.P. Koltermann, Recent deep water changes at the western boundary of the subpolar North Atlantic. To be submitted.

Weiss, R.F., J.L. Bullister, R.H. Gammon, and M.J. Warner, Atmospheric chlorofluoromethanes in the deep equatorial Atlantic. *Nature* 314, 608-610, 1985

### **Acknowledgements**

Thanks to Captain Kull and his crew for their professional assistance and their invaluable contributions to the receptions and ship tours carried out in Recife and Pointe a Pitre as part of the ‚Jahr der Geowissenschaften‘.

Meteor M53/3		CTD Stations					Page 1		
Prof.	Stat.	Date	Time	Latitude	Longitude	Water Depth	Profile Depth	Comment	
1	0	2002/06/08	13:35	4° 21.83' S	35° 52.90' W	2575	2519		
2	329	2002/06/09	12:07	2° 6.95' S	40° 0.03' W	1288	1298		
3	330	2002/06/09	15:26	2° 1.94' S	40° 0.07' W	2434	2397		
4	331	2002/06/09	18:14	1° 51.79' S	39° 59.66' W	3363	3283	Stop due to malfunct. echo sounder	
5	332	2002/06/09	21:38	1° 38.48' S	39° 59.30' W	3671	3663		
6	333	2002/06/10	01:51	1° 16.88' S	39° 59.15' W	3777	3750		
7	334	2002/06/10	06:30	0° 50.80' S	39° 59.37' W	3885	3867		
8	335	2002/06/10	11:01	0° 25.57' S	39° 59.53' W	3986	3976		
9	336	2002/06/10	16:03	0° 0.16' S	39° 59.87' W	3479	3439		
10	337	2002/06/10	20:32	0° 24.80' N	39° 59.97' W	3361	3237		
11	338	2002/06/11	00:56	0° 50.14' N	40° 0.01' W	4404	4394		
12	339	2002/06/11	06:15	1° 15.00' N	40° 0.19' W	4439	4388		
13	340	2002/06/11	11:39	1° 40.01' N	39° 59.82' W	4448	4400		
14	341	2002/06/11	16:53	2° 5.03' N	40° 0.47' W	4443	4419		
15	342	2002/06/11	22:08	2° 30.02' N	40° 0.35' W	4449	4428		
16	343	2002/06/12	03:52	3° 0.14' N	40° 0.16' W	4372	4324		
17	344	2002/06/12	09:26	3° 30.00' N	40° 0.00' W	4331	4259		
18	345	2002/06/12	15:16	4° 0.00' N	40° 0.01' W	4234	4218		
19	346	2002/06/12	20:36	4° 30.00' N	40° 0.02' W	4547	4534		
20	347	2002/06/13	02:14	5° 0.01' N	39° 59.93' W	4584	4517		
21	348	2002/06/13	07:55	5° 30.02' N	40° 0.03' W	4676	4658		
22	349	2002/06/13	13:41	6° 0.00' N	40° 0.10' W	4618	4597		
23	350	2002/06/13	21:56	6° 29.03' N	39° 27.01' W	4821	4808		
24	351	2002/06/14	05:21	6° 53.95' N	38° 56.38' W	4430	4457		
25	352	2002/06/14	13:13	7° 26.84' N	38° 19.32' W	4833	4843		
26	353	2002/06/14	20:18	7° 27.13' N	37° 47.51' W	4813	4686		
27	354	2002/06/15	01:49	7° 27.81' N	37° 19.13' W	4812	4759		
28	355	2002/06/15	07:08	7° 28.64' N	36° 52.39' W	4813	4524	Water depth uncertain	
29	356	2002/06/15	12:39	7° 28.40' N	36° 49.96' W	4300	3155	Stop due to probl. with data acquisition	
30	357	2002/06/16	12:41	7° 25.02' N	34° 17.33' W	4700	4682		
31	359	2002/06/21	00:12	15° 14.43' N	51° 21.05' W	4346	4295		
32	360	2002/06/21	04:41	15° 16.84' N	51° 42.22' W	5417	4868	Due to LADCP stop at 5000 dbar	
33	361	2002/06/21	09:28	15° 19.29' N	52° 3.53' W	4960	4968		
34	362	2002/06/21	14:16	15° 21.84' N	52° 24.68' W	5165	4910	Due to LADCP stop at 5000 dbar	
35	363	2002/06/21	18:56	15° 24.37' N	52° 45.93' W	5132	5154		

Meteor M53/3		CTD Stations					Page 2		
Prof.	Stat.	Date	Time	Latitude	Longitude	Water Depth	Profile Depth	Comment	
36	364	2002/06/21	23:42	15° 26.82' N	53° 7.07' W	5266	2066	Stop due to malfunct. cond. sensor	
37	364	2002/06/22	01:11	15° 26.78' N	53° 7.01' W	5271	5262		
38	365	2002/06/22	06:10	15° 29.14' N	53° 28.28' W	5403	5422		
39	366	2002/06/22	11:05	15° 31.68' N	53° 49.48' W	5470	4912		
40	367	2002/06/22	15:58	15° 34.23' N	54° 10.71' W	5445	5459		
41	368	2002/06/22	20:52	15° 36.65' N	54° 31.82' W	5449	4905	Due to LADCP stop at 5000 dbar	
42	369	2002/06/23	02:22	15° 39.09' N	54° 53.03' W	5486	5501		
43	370	2002/06/23	07:25	15° 41.63' N	55° 14.27' W	5488	4904	Due to LADCP stop at 5000 dbar	
44	371	2002/06/23	12:22	15° 44.10' N	55° 35.45' W	5480	5497		
45	372	2002/06/23	17:10	15° 46.55' N	55° 54.08' W	5455	4904	Due to LADCP stop at 5000 dbar	
46	373	2002/06/23	22:12	15° 49.02' N	56° 17.85' W	5326	5335		
47	374	2002/06/24	03:10	15° 51.57' N	56° 38.94' W	5282	4906	Due to LADCP stop at 5000 dbar	
48	376	2002/06/24	21:45	15° 54.17' N	57° 0.05' W	5165	5190		
49	377	2002/06/25	02:50	15° 56.45' N	57° 21.41' W	5282	290	Stop due to probl. with data acquisition	
50	377	2002/06/25	03:23	15° 56.43' N	57° 21.36' W	5283	5291		
51	378	2002/06/25	09:09	15° 58.92' N	57° 42.61' W	5404	5426		
52	379	2002/06/25	14:33	16° 1.49' N	58° 4.07' W	5360	4905	Due to LADCP stop at 5000 dbar	
53	380	2002/06/25	19:30	16° 3.92' N	58° 25.49' W	5588	5603		
54	381	2002/06/26	00:52	16° 6.31' N	58° 46.68' W	5750	4906	Due to LADCP stop at 5000 dbar	
55	382	2002/06/26	06:24	16° 10.39' N	59° 16.44' W	5017	4905	Due to LADCP stop at 5000 dbar	
56	383	2002/06/26	11:54	16° 14.29' N	59° 46.94' W	5070	4905	Due to LADCP stop at 5000 dbar	
57	385	2002/06/26	22:52	16° 16.25' N	60° 16.44' W	4822	4854		
58	386	2002/06/27	03:00	16° 18.77' N	60° 31.50' W	4649	4691		
59	387	2002/06/27	06:44	16° 17.63' N	60° 34.45' W	3494	3465		
60	388	2002/06/27	09:13	16° 17.70' N	60° 36.66' W	2891	2971		
61	389	2002/06/27	11:20	16° 17.64' N	60° 38.05' W	2475	2177	Water depth uncertain	
62	390	2002/06/27	13:13	16° 17.45' N	60° 40.99' W	1726	1685		
63	391	2002/06/27	15:09	16° 17.43' N	60° 45.14' W	1026	1021		
64	393	2002/06/28	06:35	15° 39.78' N	61° 26.53' W	562	561		
65	394	2002/06/28	07:35	15° 41.89' N	61° 27.53' W	1079	1050		
66	395	2002/06/28	08:54	15° 45.24' N	61° 28.59' W	695	696		
67	396	2002/06/28	09:56	15° 47.97' N	61° 29.71' W	479	468		
68	397	2002/06/28	11:18	15° 57.24' N	61° 33.48' W	258	246		
69	398	2002/06/28	20:22	14° 56.83' N	61° 9.15' W	420	403		
70	399	2002/06/28	21:18	15° 0.07' N	61° 10.79' W	612	597		

Meteor M53/3		CTD Stations					Page 3		
Prof.	Stat.	Date	Time	Latitude	Longitude	Water Depth	Profile Depth	Comment	
71	400	2002/06/28	22:18	15° 3.46' N	61° 12.56' W	1500	1456		
72	401	2002/06/28	23:52	15° 6.04' N	61° 13.79' W	2046	2026		
73	402	2002/06/29	09:45	15° 9.09' N	61° 15.26' W	1457	1446		
74	403	2002/06/29	11:26	15° 12.23' N	61° 16.87' W	687	666		
75	403	2002/06/29	20:12	14° 10.91' N	60° 54.18' W	452	440		
76	405	2002/06/29	21:02	14° 13.07' N	60° 53.83' W	782	754		
77	406	2002/06/29	22:00	14° 15.60' N	60° 53.20' W	879	882		
78	407	2002/06/29	23:14	14° 18.78' N	60° 52.75' W	754	805		
79	408	2002/06/30	00:26	14° 21.62' N	60° 52.38' W	358	360		
80	409	2002/06/30	14:28	13° 36.68' N	60° 56.01' W	382	385		
81	410	2002/06/30	15:31	13° 32.99' N	60° 58.67' W	333	331		
82	411	2002/06/30	16:18	13° 30.59' N	61° 0.35' W	373	360		
83	412	2002/06/30	17:12	13° 27.90' N	61° 2.14' W	865	840		
84	413	2002/06/30	18:32	13° 25.11' N	61° 4.27' W	1000	1047		
85	413	2002/06/30	19:45	13° 23.31' N	61° 5.58' W	480	493		
86	415	2002/06/30	21:56	13° 9.90' N	61° 4.19' W	431	402		
87	416	2002/06/30	23:55	12° 57.91' N	61° 0.85' W	636	637		
88	417	2002/07/01	01:15	12° 53.59' N	60° 59.82' W	1128	1131		
89	418	2002/07/01	03:59	12° 38.56' N	60° 56.23' W	1348	1307		
90	419	2002/07/01	06:51	12° 23.06' N	60° 52.32' W	2000	1931		
91	420	2002/07/01	10:09	12° 7.88' N	60° 48.13' W	2328	690	Due to bottom alarm stop at 652 dbar	
92	421	2002/07/01	13:05	11° 50.10' N	60° 43.69' W	1727	1651		
93	422	2002/07/01	16:25	11° 33.29' N	60° 39.76' W	673	648		
94	423	2002/07/01	18:00	11° 42.61' N	60° 38.17' W	1170	1166		
95	424	2002/07/01	20:45	11° 58.78' N	60° 38.38' W	2337	2231		
96	425	2002/07/01	23:30	12° 15.30' N	60° 38.99' W	2324	2299		
97	426	2002/07/02	02:19	12° 32.06' N	60° 39.30' W	2444	2404		
98	427	2002/07/02	05:20	12° 48.64' N	60° 40.06' W	2317	2285		
99	428	2002/07/02	08:33	13° 4.94' N	60° 40.63' W	2127	2076		
100	429	2002/07/02	11:24	13° 21.44' N	60° 41.24' W	1670	1631		
101	430	2002/07/02	14:01	13° 38.09' N	60° 41.68' W	1204	1177		
102	431	2002/07/02	16:25	13° 54.60' N	60° 42.39' W	1120	1058		
103	432	2002/07/02	18:48	14° 11.02' N	60° 42.22' W	1278	1251		
104	433	2002/07/02	20:15	14° 15.84' N	60° 42.05' W	1414	1405		
105	434	2002/07/02	22:26	14° 27.46' N	60° 42.02' W	1100	1158		

<b>Meteor M53/3</b>		<b>CTD Stations</b>				<b>Page 4</b>		
Prof.	Stat.	Date	Time	Latitude	Longitude	Water Depth	Profile Depth	Comment
106	435	2002/07/03	01:00	14° 43.61' N	60° 41.80' W	674	663	
107	436	2002/07/03	03:43	15° 0.07' N	60° 41.84' W	1000	985	
108	437	2002/07/03	06:09	15° 16.21' N	60° 41.64' W	2070	2020	
109	438	2002/07/03	09:15	15° 32.62' N	60° 41.52' W	2593	2569	
110	439	2002/07/03	12:46	15° 48.98' N	60° 41.43' W	1640	1621	
111	440	2002/07/03	15:22	16° 5.34' N	60° 41.19' W	1200	1194	

**Table 3-1 Moorings: Location, Water depths, Dates**

Name	Latitude	Longitude	Depth	Deployment Date	Retrieval Date
B1	7°28.40'N	36°50.00'W	4510m	15.6.2002, 16:05	
B2	7°24.70'N	34°17.30'W	4690m	16.6.2002, 17:27	

**Table 3-2 Mooring B1**

Instrument	Number	Depth	Comments
Releaser	SN798	4455m	
Releaser	SN 517	4455m	
RCM11	94	4449m	
MicroCat C,T	1888	4448m	
MicroCat C,T	1915	4147m	
RCM11+P	93	4145m	
MicroCat C,T	1931	3839m	
RCM11+P	92	3838m	

Sampling rate for all instruments : 30min.

RCM: Andraea Acoustic Current Meter, +P: with pressure sensor

MicroCat C,T : SBE, measurement of temperature and conductivity

Radio frequency: 160.785 MHz

**Table 3-3 Mooring B2**

Instrument	Number	Depth	Comments
Releaser	AR810	4655m	
Releaser	RT238	4655m	
RCM11	97	4654m	
MicroCat C,T	1936	4648m	
MicroCat C,T	1934	4347m	
RCM11+P	91	4345m	
MicroCat C,T	1932	4039m	
RCM11+P	89	4033m	

Sampling rate for all instruments: 30min

Radio frequency: 160.725 MHz